Progress In Electromagnetics Research C, Vol. 127, 251–261, 2022

A Multi-Objective Array Pattern Optimization via Thinning Approach

Ahmed J. Abdulqader[1, *], Awan N. Mahmood[1], and Yessar E. Mohammed Ali[2]

Abstract—In this paper, the possibility of synthesizing a linear antenna array for multiple objectives with the thinning approach is demonstrated. The thinning space is constrained to three cases (side, central, and random) parts instead of a fully filled linear array. In the case of the side part, a set of elements located on both edges of the array are removed with the optimized elements close to the center remaining unchanged. As in the case of the central part, only a set of elements close to the center are removed. In the case of a random selection of elements, the cancellation process is carried out randomly within the sides and the center. Since the amplitude weights of the elements located on the edges of the array have a small amplitude excitation, the method of side thinning gives better results than the other two cases. Moreover, in cases of side and random thinning, the last element of each side is excluded from the thinning process to maintain the aperture size. The convex algorithm (CA) is used to perform such thinning optimization. CA optimization efficiently computes a multi-objective function in coordination with the thinned array technique, such as preserving the main beamwidth in all cases with the reduction of sidelobe levels, generating one or more nulls, and steering the main beam in a certain direction. The simulation results, in all cases, show that 30%–40% of the array elements can be turned off with achieving a multi-objective radiation pattern.

1. INTRODUCTION

The elimination of radiating components from a regularly spaced or cyclic array to generate the desired radiation pattern is referred to as array thinning. The main objective of thinning is to reduce the weight, cost, energy consumption, and execution time of the algorithm [1–3]. The locations of the radiating elements will be determined in thinning array synthesis, and each element will have two states: "ON component" or "active state" (when the element is supplied) and "OFF component" or "passive state" (when the elements are passively removed or not fed by the source) [4].

A thinning array can be categorized into two main types: one that the array elements can be placed anywhere in the array aperture, and the other that the distances between elements in the array aperture are evenly spaced [5]. In the first state, some of the elements can be placed arbitrarily, and therefore there will be continuous changes in the locations of these elements, while in the second state, the elements can be placed in the antenna array aperture, and therefore, its search space is separate and specific [5]. However, when the number of array elements is to be increased up to hundreds, the search space for the combinatorial optimization problem is greatly increased, which causes a big problem for traditional and numerical optimization algorithms [6]. Here, the number of elements in the array aperture must be reduced while maintaining the desired radiation characteristics of the reference structures with modification; therefore, many optimization methods have been successfully investigated to implement the idea of thinning techniques [7, 8]. Using these approaches led to important

Received 19 October 2022, Accepted 14 December 2022, Scheduled 19 December 2022
* Corresponding author: Ahmed Jameel Abdulqader (ah_8611@yahoo.com).
[1] College of Electronics Engineering, Ninevah University, Mosul-41002, Iraq. [2] Department of Computer and Communications Engineering, College of Engineering, Nawroz University, Duhok-42001, Iraq.

developments, especially using global optimization methods [9]. Some approaches, such as differential evolution (DE) [10, 11], genetic algorithm (GA) [12], ant colony optimization (ACO) [13], particle swarm optimization (PSO) [14, 15], and compressed sensing [16], have indeed been utilized to synthesize thinning arrays for many applications.

There are several challenges in using thinning arrays to simplify the array system, including a change in the electromagnetic properties of the original array. One of the most important characteristics is the change in directivity and beamwidth, in addition to that, the loss of control of the side lobes due to turn off a group of elements. Another challenge is the inability to turn off the elements located in the center of the array. When the center elements are turned off, the radiation pattern will be completely destroyed, and therefore control over it will be lost with the presence of the side elements only, as these elements have low weight values, which leads to their inability to be used in the required modern applications. a distortion of the radiation pattern completely [17–19].

In this paper, the thinning process is applied adaptively in three cases according to the indexing of the elements in the array, where the indexes are selected into the side, center, and random locations based on their amplitude-only weights. As for the amplitude weights taper, usually, the center elements have high amplitude weights, while the side elements have small excitations. Thus, some of the elements with small amplitudes excitation, whether in the center or side locations, can be turned off without undesirable changes in the characteristics of the original radiation pattern. CA is used to remove some elements that are less effective than others in different locations so that the overall performance of the array is not reduced much compared to the performance of the original fully filled array. In each case, when some of the elements are selected to be removed, other elements are kept unchanged, and thus the thinned array has some properties similar to the original array. Also, to keep the size of the resulting thinned array equal to the size of the original un-thinned array, the last element at both ends of the linear array is excluded from the thinning process. Moreover, although the structure of the thinning array differs from the structure of the original filled array in some cases, the beamwidth of the proposed thinning array remains equal to that of the original beamwidth. Furthermore, the thinning array enjoys several advantages such as a rather fast convergence time and a simple excitation network; therefore, this array can be used in MIMO applications in the fifth generation and WiFi applications.

This article applies a thinning array to achieve a multi-objective problem. A set of trade-off curves are provided for several characteristics of beam-pattern in a thinning array. These characteristics mention a set of given beam pattern properties such as controlling the beamwidth, generation of several null steering, controlling of the null width, and other properties as a function of sidelobe level reduction. Thus, this information will allow the antenna array designers to meet the requirements of the high gain of wireless communication systems by using a small number of active elements.

2. MODEL OF MULTI-OBJECTIVE FUNCTION WITH THINNED METHOD

Figure 1 shows the right side of the general structure of the standard linear array that consists of N elements, then the standard array factor (AF) in the far field can be written as [3]:

$$AF(u) = 2\sum_{n=1}^{N} w_n e^{j\frac{2\pi}{2}(n-1)d_n u} \tag{1}$$

where $w_n \in C^N$, for $n = 1, 2, \ldots, N$, is complex weights that include both amplitudes and phases of the elements in a linear array; d is the distance between any two successive elements; $u = \sin\theta$ is the main beam scanning angle. Usually, in the thinning process, amplitude-only weighting is used to excite the elements and also to reduce the complexity of the array system, so $w_n = |w_n|$. Regarding the excitation amplitude of the original filled array before using the thinned method, it is important to choose a suitable distribution by optimizing all the elements using algorithms or polyominos such as Taylor or Dolph, or other methods. Usually, these distribution generations are arranged with high weights in the center (middle) and low weights at the sides (edges). According to this distribution, the elements of the initial array can be divided into two parts. The first is a central-part linear array, which contains some elements distributed in the middle of the array, and their weights have high values, while the second is a side-part linear array, which includes elements close to the edges, and their weights have low values.

The number of elements in the two parts is determined by the designer, where the center elements are calculated from $N-2K$, while the sides are from $N-2K+1$, where K is the number of side elements (see Figure 2).

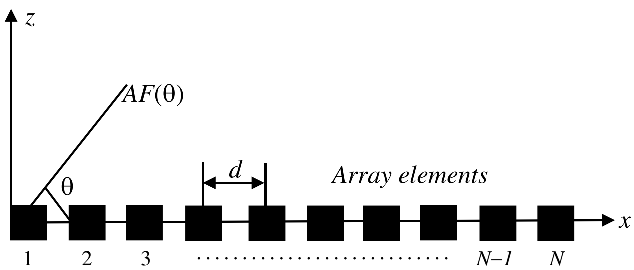

Figure 1. Right side of general structure of the standard linear array.

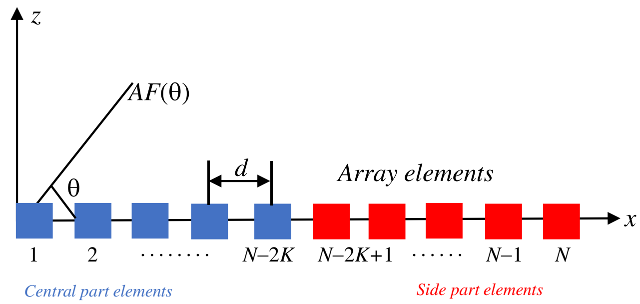

Figure 2. Details of central and side parts in the right side of general structure of the standard linear array.

Then, the array factor of these two parts combined can be written as:

$$AF(u) = \underbrace{\sum_{n=1}^{N-2K} C_n \left|w_n\right| e^{j\frac{2\pi}{2}(n-1)d_n u}}_{\text{Central-part linear array}} + \underbrace{\sum_{n=N-2K+1}^{N} S_n \left|w_n\right| e^{j\frac{2\pi}{2}(n-1)d_n u}}_{\text{Side-part linear array}} \tag{2}$$

where C_n and S_n are partial vectors, and they will be used to determine which of the elements in the two parts are in the active (ON) or passive (OFF) state. In the case of fully optimized elements (i.e., all elements are in active state), the two vectors C_n and S_n must have all of their values as ones. These two vectors must be optimized to find the most suitable group of active elements in either the central or side or randomly. To do this, CA is used under the following constraint:

$$\begin{aligned} &\min\{AF([C_n \text{ or } S_n],\ |w_n|)\} \\ &s.t.,\ [C_n \text{ or } S_n] \in \{0,1\} \end{aligned} \tag{3}$$

where $s.t.$ means subject to. This constraint assigns C_n and S_n values to a set of zeros and ones randomly based on the optimization process. Then the new weights become $|w_{new}| = [C_n|w_n|S_n|w_n|]$.

The design of the main beam constraints is

$$lB \le |AF(u)| \le uB, \quad u \in [-1,1] \tag{4}$$

where lB and uB are constants, and they represent the response limits of lower and upper bounds, respectively. Through this constraint, the width of the main beam is controlled. It is possible to rewrite the constrain in (4) as:

$$lB \le |S(u)|w_{new}|| \le uB \tag{5}$$

where:

$$S(u) = \left[e^{j\frac{2\pi}{2}(n-1)d_1 u} + e^{j\frac{2\pi}{2}(N-2K+1)d_1 u}\right] + \left[e^{j\frac{2\pi}{2}(n-1)d_2 u} + e^{j\frac{2\pi}{2}(N-2K)d_2 u}\right] + \ldots \tag{6}$$

is the vector manifold of a linear array. The constraint shown in (5) is pairs of linear inequalities in $|w_{new}|$; therefore, $|w_n|$ is convex, and it is easy to introduce other constraints to achieve multi-objectives of the desired pattern. The constraint shown in (5) provides direct control of the main beam region (MBR) in (7a) and the modification of the side lobe region (SLR) (7b), as well as the null regions (NRs) (7c) as follows:

$$\min |w_n|\delta \tag{7}$$

$$s.t. \quad lB \le |S(u)|w_n|| \le uB, \quad \{u\} \in MLR \tag{7a}$$

$$|S(u)|w_n|| \le \delta, \quad \{u\} \in SLR \tag{7b}$$

$$|S(u)|w_n|| \le \delta_n, \quad \{u\} \in NR_s \tag{7c}$$

Although the goal of this paper is to develop a thinned linear array method, for the sake of completeness, an important aggregation objective (achievement of several objectives with controlling of beam width) is briefly presented in (7). The problem in (7) minimizes delta which represents the value of the response of SLR. Although other properties of the beam pattern may be controlled, δ_n is a parameter specified by the designer that expresses the value of the response of NRs. Figure 3 shows the flowchart of the proposed thinning model.

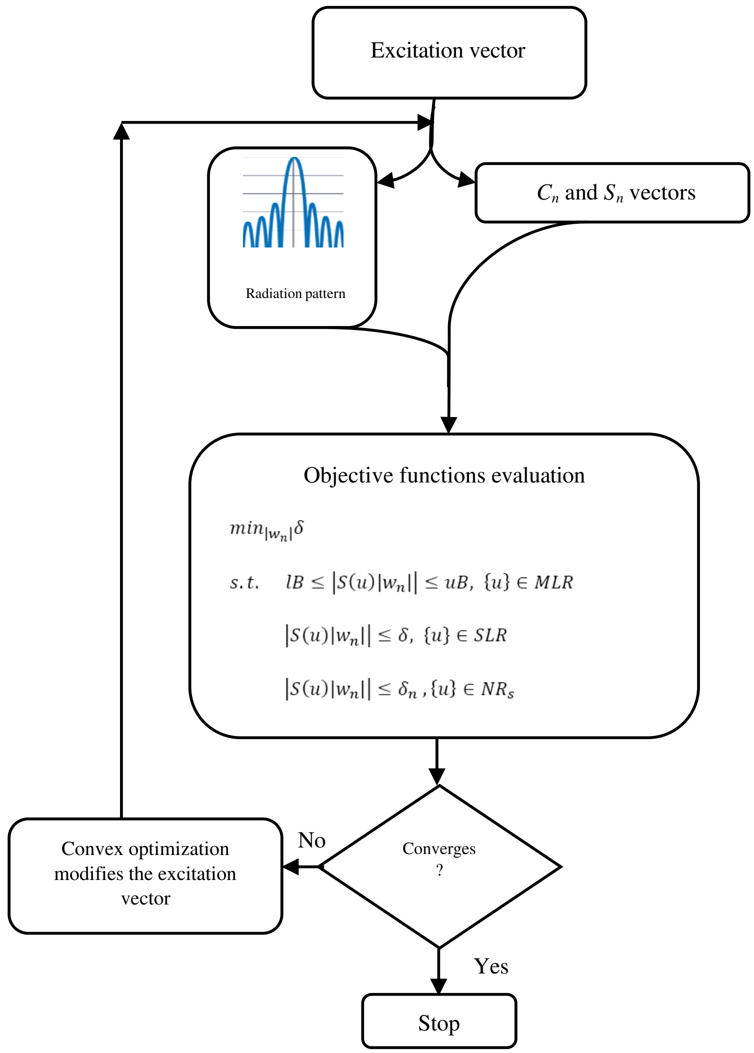

Figure 3. Flowchart of the proposed thinning model.

3. SIMULATION RESULTS

In this section, several simulation results are presented and realized to make a useful performance comparison of the proposed methods for constructing a thinned array with multi-objective functions. In all experiments, a linear array with $N = 40$ elements was considered with the elements placed symmetrically around the center and spaced by half a wavelength. Such a fully non-thinned array is then portioned into two-part arrays with dimensions $N - 2K$ and $2K(N - K)$, where K represents the number of side-part array elements. The following tests were taken to verify the performance of the thinned array with a multi-objective function.

In the first test, applying a thinning process to the side part of a linear array, which contains K elements, is discussed. CA is used to determine which elements within the $N - K - 1$ side group should be optimally turned off to achieve multiple goals. To study the possibility of achieving several objectives in the desired pattern with the thinning process, the required beam width is initially determined at 4 degrees with the possibility of adaptively reducing the side lobes. In this case, selecting the number of elements needed to be removed from the side part is done by the algorithm adaptively, where it is possible to turn off up to 9 elements from each side, except for the last element, i.e., 18 elements are removed from the main array while the elements of the central part remain in the ON state. The level of the sidelobes depends on the number of OFF elements, and as the number of OFF elements increases, the level of the sidelobes also increases and vice versa. Figure 4 shows the radiation pattern of the partially thinned linear array with the corresponding distribution of amplitude weights. It can be seen from this figure that 7 elements were turned off from each side, and the level of the sidelobes was $-19\,\text{dB}$. For the same number of turned-off elements, one or more broad nulls can be generated. Figure 5 shows the optimized radiation pattern with a wide null centered at 50°, by a width of more than 10° with a depth of $-80\,\text{dB}$ while keeping the width of the main beam at the desired value. The process of generating one or more broad nulls is related to the level of the sidelobes.

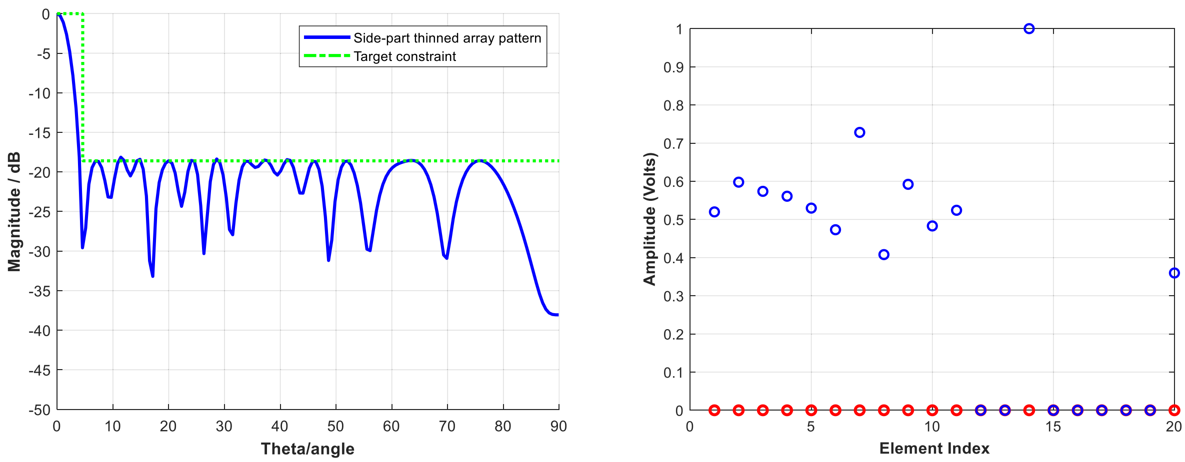

(a) (b)

Figure 4. Optimized side-part thinned array pattern and, (a) ON (blue color) and (b) OFF (red color) elements distributions.

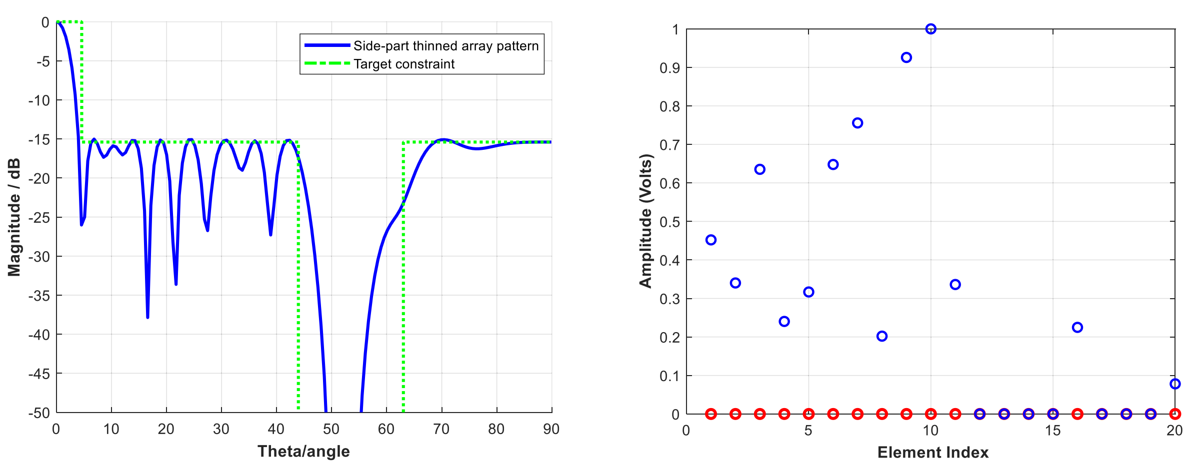

(a) (b)

Figure 5. Optimized side-part thinned array pattern with wide null steering and, (a) ON (blue color) and (b) OFF (red color) elements distributions.

The complexity percentage of the feeding network may be defined by the ratio of the number of active elements ($2N$-number of OFF elements) to the total number of elements:

$$Complexity\ percentage = \frac{total\ numer\ of\ elements(2N) - \#OFF\ elements\ in\ both\ sides}{2N} * 100\% \quad (8)$$

The complexity percentage, in this case, is 65% (the number of OFF elements on each side is 7). The main beam can also be steered by changing θ in u to the desired angle for the same number of OFF elements. Figure 6 represents the radiation pattern under the following specifications: beam steered at 30° and sidelobe level at -19 dB.

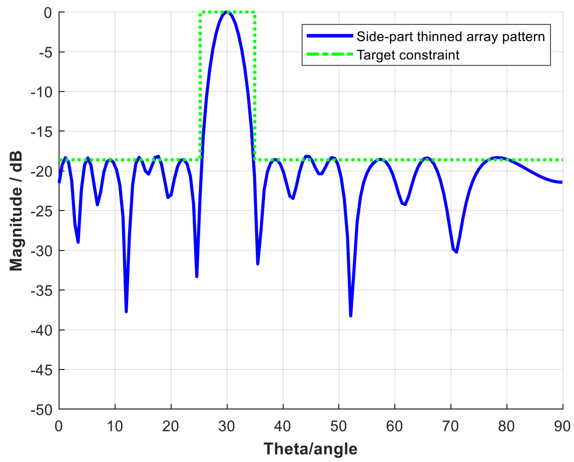

Figure 6. Optimized side-part thinned array pattern with main beam steering at 30 deg.

We mean that the radiation pattern was preserved in the case of turning off some elements in the center, and this matter was .

In the second test, adding the thinning process to the center section of a linear array containing $2(N - K)$ elements is presented. Also, CA is responsible for determining which element is turned off. The new challenge in this section is that some elements are stopped in the center of the array, despite having high exciting weights compared to the weights of the side elements. This case (the radiation pattern was preserved in the case of turning off some elements in the center) solves the problems which were not achieved by other researchers, e.g., [18, 19]. Using the constraints shown in (7), this case was achieved, but due to the low weights of the side elements, the reduction of the side lobes is difficult compared to the case of thinning the side elements. The weights of the side elements are relied upon with some active center elements to achieve the multi-objectives of the radiation pattern. The maximum number of center elements that are set to be eliminated in this test is 10 elements to have the minimum beam pattern requirement, and reducing the number of OFF elements in the center by less than 12 leads to better results.

Figure 7 shows the construction of a beam pattern by removing 10 elements from the center, where a sidelobe level of -15 dB was obtained while keeping the width of the main beam the same as in the case of a fully filled array. The percentage complexity, in this case, is 75%. Figure 8 shows the generation of null steering focused at 50 degrees and a width of more than 10 degrees at the same test. Also, it is possible to steer the main beam at a certain angle (see Figure 9). It is observed through these figures that there is an increase in the sidelobe levels more than in the first test, but the level of these lobes is still under the required limit, and it is sufficient to cancel any interference signal.

In the third test, the performance of the proposed thinned array is considered by randomly removing some elements in the aperture, i.e., some elements are set to turn off from the center and the sides except for the last element from each side to keep the original size of the array unchanged. Figures 10, 11, and 12 show applying the random method to construct the multi-objective beam pattern.

To make an efficient comparison among the three tests, Figure 13 shows the resulting patterns of these tests with the corresponding amplitude weights. It is noticed from this figure that removing some

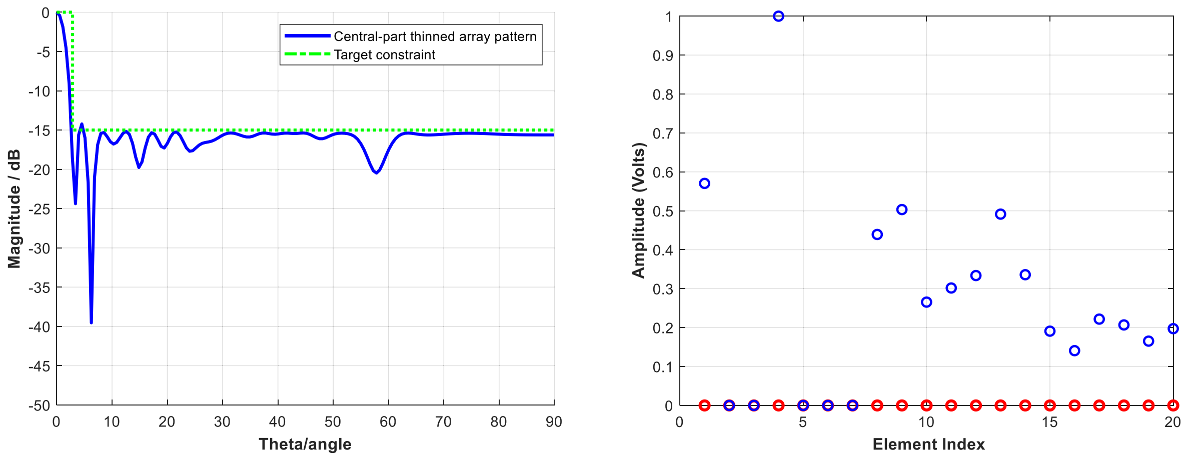

(a) (b)

Figure 7. Optimized central-part thinned array pattern and (a) ON (blue color) and (b) OFF (red color) elements distributions.

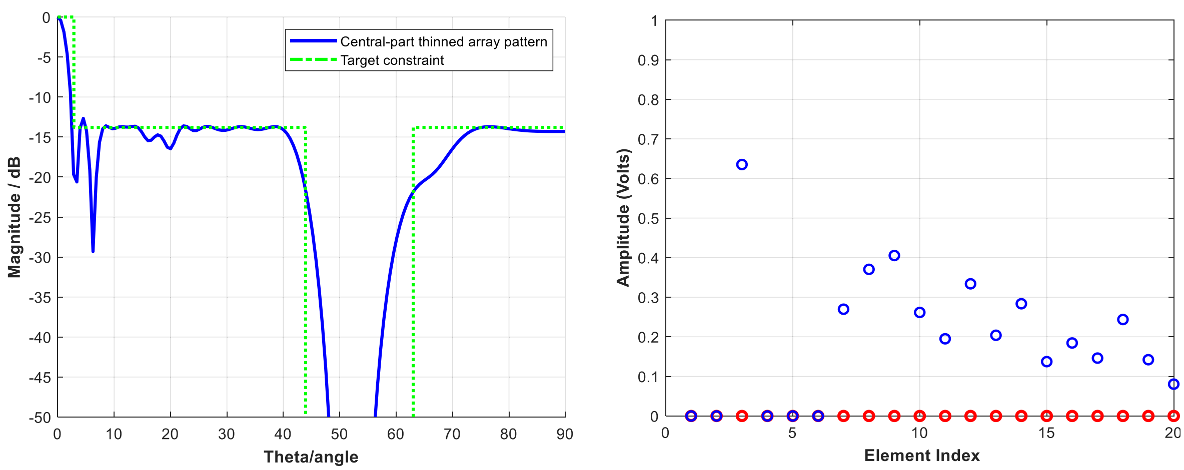

(a) (b)

Figure 8. Optimized central-part thinned array pattern with wide null steering and (a) ON (blue color) and (b) OFF (red color) elements distributions.

elements from the sides is better than the other two methods with the effectiveness of the other two methods in practical terms. In all the tests, the width of the main beam was controlled at 4 degrees with a difference in the level of the sidelobes, which indicates the effectiveness of the proposed method by us.

Finally, the performance of the thinned array in terms of sidelobe levels, directivity, main beamwidth, as well as trade-off relationships among the generation of the number of nulls, the width of null, and sidelobe level as a function of the number of OFF elements are depicted in Figures 14, 15, 16, 17, and 18, respectively. From Figure 14 it is seen that increasing the number of OFF elements leads to an increase in the sidelobe levels, and this is logical, where a better result is obtained when elements are turned off from the sides. In Figures 15 and 16, the radiation pattern almost maintains the directivity and width even if half of the elements are turned off from the main array, and this is an important benefit in constructing a thinned array. As for Figure 17, it is possible to generate a set of nulls with the cancellation of some elements, but at the expense of an increase in the level of the side lobes. Also, it is possible to generate an ultrawide null up to 10 degrees with the same previous

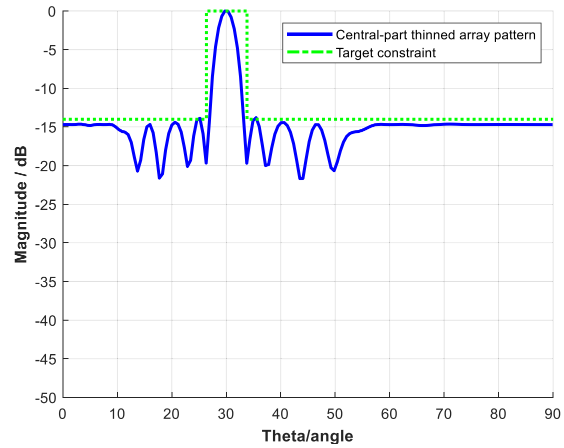

Figure 9. Optimized side-part thinned array pattern with main beam steering at 30 deg.

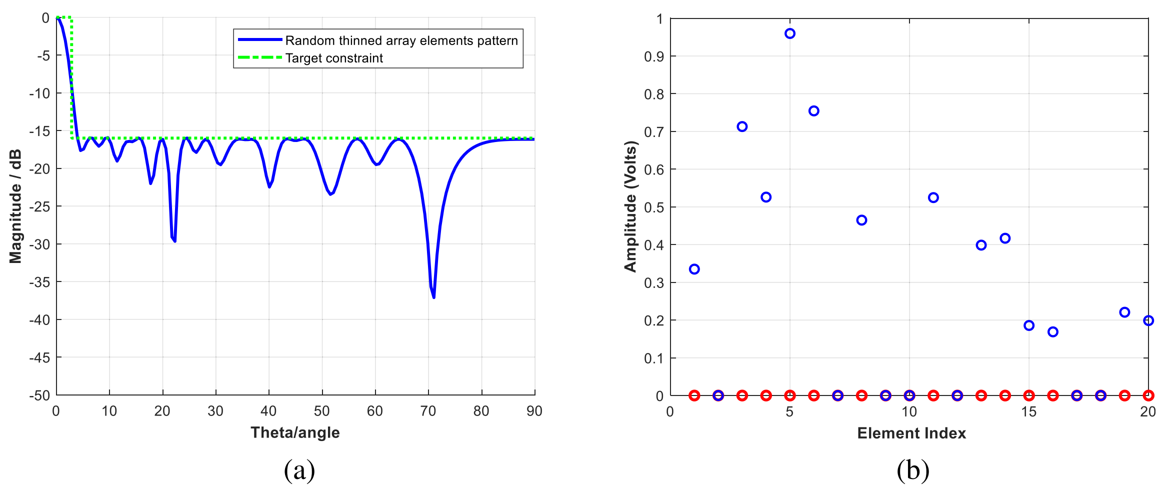

Figure 10. Optimized random thinned array elements pattern and (a) ON (blue color) and (b) OFF (red color) elements distributions.

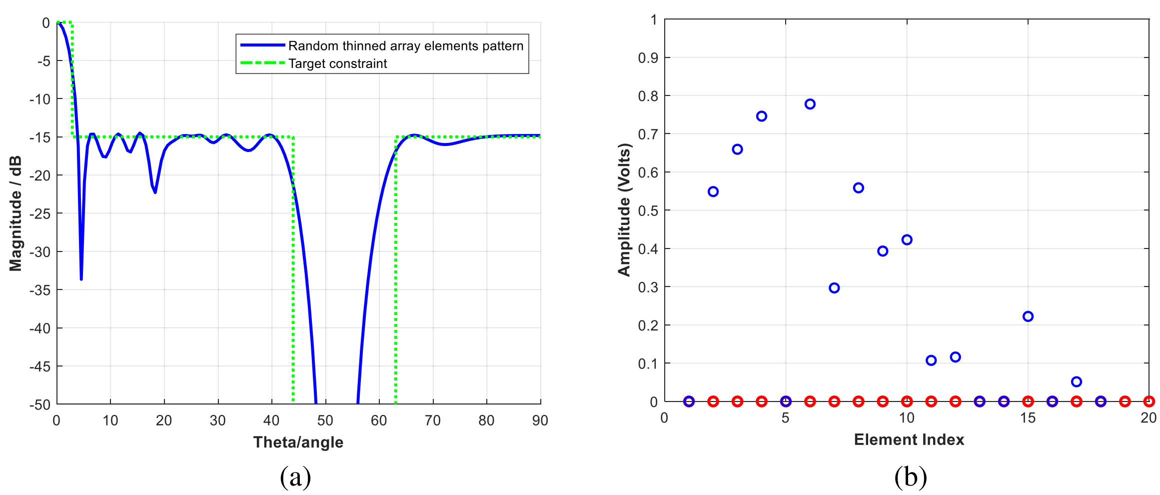

Figure 11. Optimized random thinned array elements pattern with wide null steering and (a) ON (blue color) and (b) OFF (red color) elements distributions.

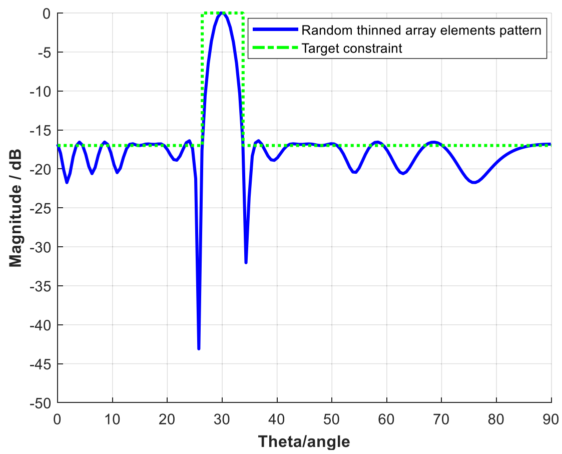

Figure 12. Optimized random thinned array elements pattern with main beam steering at 30.

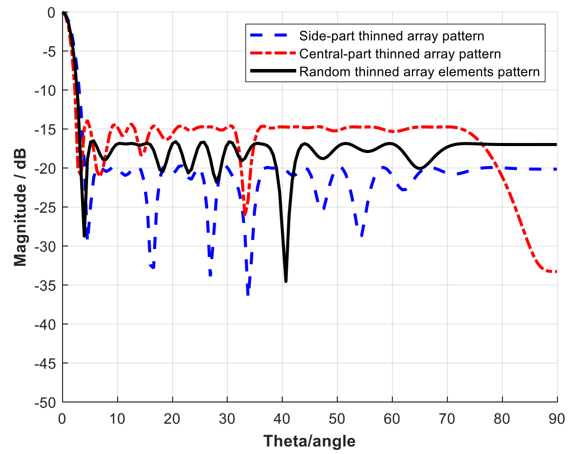

Figure 13. Optimized pattern for three cases: Side, Center and Random thinned elements.

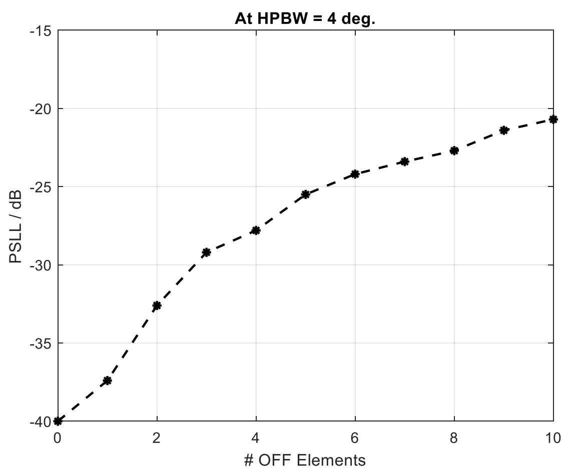

Figure 14. The PSLL with #OFF elements.

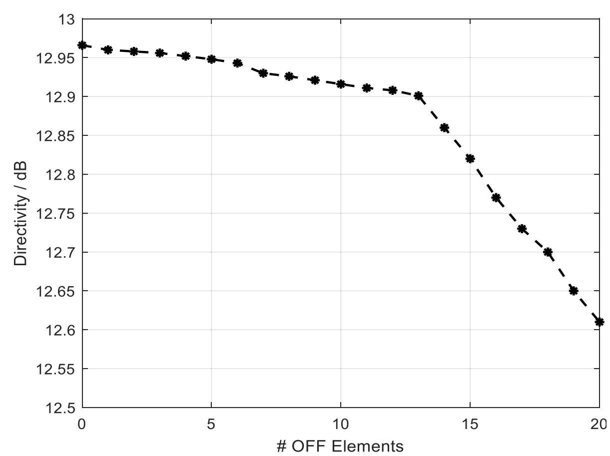

Figure 15. The directivity with #OFF elements.

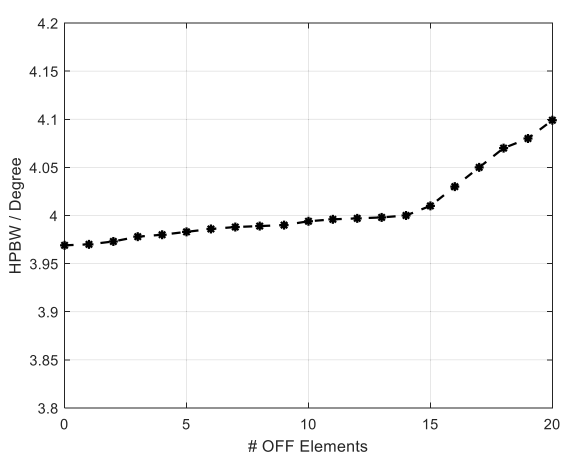

Figure 16. The main beam width with #OFF elements.

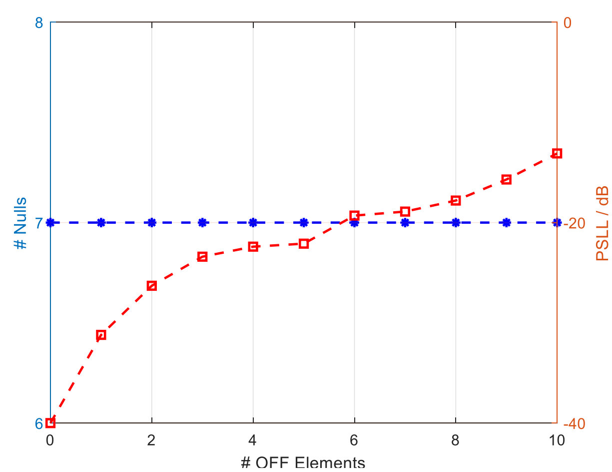

Figure 17. The trade-off curve between # of nulls and # OFF elements relative to the sidelobe level.

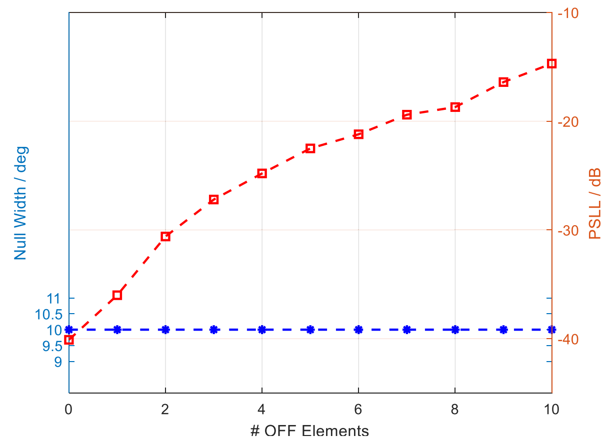

Figure 18. The trade-off curve between null width and # OFF elements relative to the sidelobe level.

trade-off relationship (see Figure 18). All of the above results achieve the effectiveness of the proposed thinning method in constructing practically acceptable radiation patterns.

4. CONCLUSION

It is clear from the simulation results that it is possible to obtain a multi-objective beam pattern for the fully filled main linear array such as controlling the main beamwidth, reducing sidelobe levels, generating one or more nulls, and steering the main beam using the partially thinned array with the least number of active elements. To optimally determine which of the elements needs to be in a passive state, the CA is used. The proposed approach constrains the search space of the optimization algorithm to a specified number of side or center elements or randomly, thus several advantages such as light weight, lower cost, and rather fast response time are obtained. When the elements are removed from the edges or randomly, the last element is excluded from the thinning process to maintain the aperture size. The tests result shows the ability of the methods used in constructing beam patterns for modern applications such as MIMO and WiFi, that require a large number of antennas.

REFERENCES

1. Fernandez-Delgado, M., J. A. Rodriguez-Gonzalez, R. Iglesias, S. Barro, and F. J. Ares-Pena, "Fast array thinning using global optimization methods," *Journal of Electromagnetic Waves and Applications*, Vol. 24, No. 16, 2259–2271, 2010.
2. Liu, Y., Z.-P. Nie, and Q. H. Liu, "A new method for the synthesis of non-uniform linear arrays with shaped power patterns," *Progress In Electromagnetics Research*, Vol. 107, 349–363, 2010.
3. Abdulqader, A. J., J. R. Mohammed, and R. H. Thaher, "Phase-only nulling with limited number of controllable elements," *Progress In Electromagnetics Research C*, Vol. 99, 167–178, 2020.
4. Wang, W.-B., Q. Feng, and D. Liu, "Synthesis of thinned linear and planar antenna arrays using binary PSO algorithm," *Progress In Electromagnetics Research*, Vol. 127, 371–387, 2012.
5. Zhang, X. and X. Zhang, "Thinning of antenna array via adaptive memetic particle swarm optimization," *J. Wireless Com. Network*, Vol. 2017, 183, 2017.
6. Li, W.-T., X.-W. Shi, and Y.-Q. Hei, "An improved particle swarm optimization algorithm for pattern synthesis of phased arrays," *Progress Electromagnetics Research*, Vol. 82, 319–332, 2008.
7. Jung, S.-H., et al., "Optimal design of thinned array using a hybrid genetic algorithm," *Journal of Electromagnetic Engineering and Science*, Vol. 21, No. 4, 261–269, 2021.
8. Oliveri, G., L. Manica, and A. Massa, "ADS-based guidelines for thinned planar arrays," *IEEE Transactions on Antennas and Propagation*, Vol. 58, 1935–1948, 2010.

9. Zaharis, Z. D., D. G. Kampitaki, P. I. Lazaridis, A. I. Papastergiou, A. T. Hatzigaidas, and P. B. Gallion, "Improving the radiation characteristics of a base station antenna array using a particle swarm optimizer," *Microwave and Optical Technology Letters*, Vol. 49, 1690–1698, 2007.
10. Li, R., L. Xu, X.-W. Shi, N. Zhang, and Z.-Q. Lv, "Improved differential evolution strategy for antenna array pattern synthesis problems," *Progress In Electromagnetics Research*, Vol. 113, 429–441, 2011.
11. Zhang, L., Y.-C. Jiao, Z.-B. Weng, and F.-S. Zhang, "Design of planar thinned arrays using a boolean differential evolution algorithm," *IET Microwaves, Antennas & Propagation*, Vol. 4, 2172–2178, 2010.
12. Abdulqader, A. J., J. R. Mohammed, and R. H. Thaher, "Antenna pattern optimization via clustered arrays," *Progress In Electromagnetics Research M*, Vol. 95, 177–187, 2020.
13. Mosca, S. and M. Ciattaglia, "Ant colony optimization applied to array thinning," *2008 IEEE Radar Conference*, 1–3, 2008.
14. Donelli, M., T. Moriyama, and M. Manekiya, "A compact switched-beam planar antenna array for wireless sensors operating at Wi-Fi band," *Progress In Electromagnetics Research C*, Vol. 83, 137–145, 2018.
15. Donelli, M. and P. Febvre, "An inexpensive reconfigurable planar array for Wi-Fi applications," *Progress In Electromagnetics Research C*, Vol. 28, 71–81, 2012.
16. Mohammed, J. R., R. H. Thaher, and A. J. Abdulqader, "Linear and planar array pattern nulling via compressed sensing," *Journal of Telecommunications and Information Technology*, 50–55, 2021.
17. Mohammed, J. R., "A method for thinning useless elements in the planar antenna arrays," *Progress In Electromagnetics Research Letters*, Vol. 97, 105–113, 2021.
18. Mohammed, J. R., "Thinning a subset of selected elements for null steering using binary genetic algorithm," *Progress In Electromagnetics Research M*, Vol. 67, 147–155, 2018.
19. Mohammed, J. R. and A. J. Abdulqader, "Array pattern restoration under defective elements," *Progress In Electromagnetics Research C*, Vol. 123, 17–26, 2022.